BIOCHEMISTRY
including biophysical chemistry & molecular biology

Article

pubs.acs.org/biochemistry

DNA Translocation by Human Uracil DNA Glycosylase: Role of DNA Phosphate Charge

Joseph D. Schonhoft, John G. Kosowicz, and James T. Stivers*

Department of Pharmacology and Molecular Sciences, The Johns Hopkins University School of Medicine, 725 North Wolfe Street, Baltimore, Maryland 21205-2185, United States

Supporting Information

ABSTRACT: Human DNA repair glycosylases must encounter and inspect each DNA base in the genome to discover damaged bases that may be present at a density of <1 in 10 million normal base pairs. This remarkable example of specific molecular recognition requires a reduced dimensionality search process (facilitated diffusion) that involves both hopping and sliding along the DNA chain. Despite the widely accepted importance of facilitated diffusion in protein−DNA interactions, the molecular features of DNA that influence hopping and sliding are poorly understood. Here we explore the role of the charged DNA phosphate backbone in sliding and hopping by human uracil DNA glycosylase (hUNG), which is an exemplar that efficiently locates rare uracil bases in both double-stranded DNA and single-stranded DNA. Substitution of neutral methylphosphonate groups for anionic DNA phosphate groups weakened nonspecific DNA binding affinity by 0.4−0.5 kcal/mol per substitution. In contrast, sliding of hUNG between uracil sites embedded in duplex and single-stranded DNA substrates persisted unabated when multiple methylphosphonate linkages were inserted between the sites. Thus, a continuous phosphodiester backbone negative charge is not essential for sliding over nonspecific DNA binding sites. We consider several alternative mechanisms for these results. A model consistent with previous structural and nuclear magnetic resonance dynamic results invokes the presence of open and closed conformational states of hUNG. The open state is short-lived and has weak or nonexistent interactions with the DNA backbone that are conducive for sliding, and the populated closed state has stronger interactions with the phosphate backbone. These data suggest that the fleeting sliding form of hUNG is a distinct weakly interacting state that facilitates rapid movement along the DNA chain and resembles the transition state for DNA dissociation.

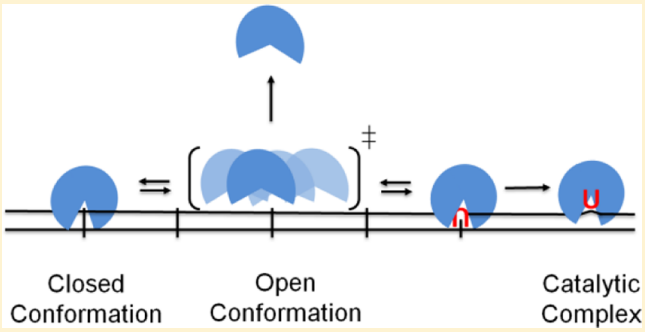

The integrity of the information content of genomic DNA depends on efficient and accurate repair of damaged DNA bases. In many cases, this task is initiated by base excision repair DNA glycosylases, which locate and cleave the glycosidic bond of rare mutagenic bases in DNA.[1,2] Unlike transcription factors or other DNA binding proteins, these unique repair glycosylases must rapidly encounter and inspect each base in the genome in the process of efficiently locating their damage targets. This unique search requirement, which is driven by the evolutionary necessity to patrol the genome, places stringent restraints on the thermodynamic and kinetic aspects of the enzyme−nucleic acid interaction that almost certainly differ from those of typical DNA binding proteins. If the glycosylase interacts too strongly with nonspecific DNA, then it spends too much time at nontarget sites; if it interacts too weakly or moves too fast, then its residence time is not long enough to allow detection of DNA damage when it is encountered. These properties of an efficient damage search are one example of what has been called the "search-speed/stability" paradox.[3,4]

To resolve the paradox, DNA glycosylases have harnessed the most favorable mechanistic features of two distinct modes of facilitated diffusion: DNA hopping and sliding.[2,3,5,6] Frequent dissociation from the DNA chain most often results in reassociation at a nearby DNA segment (hopping), keeping the enzyme from wasting time unproductively searching regions where there is no DNA and allowing it to bypass bound proteins.[7,8] Once the enzyme has encountered a new DNA segment, it then has an opportunity to remain in contact with the chain and move along it in a one-dimensional sliding mode.[3,5,6] An upper limit on the length of DNA over which sliding can occur is determined by the residence time of the enzyme on nonspecific DNA and the one-dimensional (1D) diffusion constant.[6] The importance of sliding, even over short segments of the DNA chain, is that the enzyme remains in contact with its substrate, thereby expanding the number of bases that can be inspected during each binding event. These two general modes of the search have been observed (or inferred) for many DNA glycosylases and other site-specific DNA binding proteins.[7−20]

Although the fundamental importance of hopping and sliding in the damage search is appreciated, a quantitative mechanistic

Received: November 20, 2012
Revised: February 11, 2013
Published: March 18, 2013

   dx.doi.org/10.1021/bi301561d | *Biochemistry* 2013, 52, 2526−2535

understanding of the molecular features of the DNA chain that influence an enzyme's ability to hop and slide is absent. In this regard, it is widely believed that the polyanion character of the DNA phosphate backbone provides an important nonspecific electrostatic handle allowing engagement of positively charged side chains on the enzyme. Such interactions may play a role in both hopping and sliding along nonspecific DNA, but also in other steps of the reaction such as specific recognition, making it challenging to sort out these individual effects.[21−23] Specifically, electrostatic tracking along the phosphate backbone is often invoked as the primary translocation mode for DNA sliding, but a direct test of this mechanism has been absent. Here we investigate the role of charged DNA phosphate groups in the ability of human uracil DNA glycosylase (hUNG) to hop and slide along DNA during its search for uracil bases. The results show that a continuous backbone charge is not required for hUNG to track efficiently along a DNA strand, and that the transient sliding state has features that resemble the transition state for DNA dissociation.

MATERIALS AND METHODS

Protein and Oligonucleotide Reagents. hUNG was purified as previously described.[9] Protein concentrations were determined by absorbance measurements at 280 nm using an extinction coefficient of 33.68 mM^{-1} cm^{-1}. Oligonucleotides except for those containing methylphosphonate linkages were ordered from Integrated DNA Technologies (http://www.IDTDNA.com) in the crude desalted form and purified by denaturing polyacrylamide gel electrophoresis (PAGE). All oligonucleotide sequences are reported in the Supporting Information, and concentrations were determined by UV absorption at 260 nm using extinction coefficients calculated from nearest neighbor parameters.

Experimental Conditions. All measurements in this paper and the following paper (DOI: 10.1021/bi301562n) were taken at 37 °C in a standard reaction buffer consisting of 20 mM HEPES (pH 7.5), 0.002% Brij 35 detergent (Sigma-Aldrich), 3 mM EDTA (added from a 0.5 M stock at pH 8.0), and 1 mM DTT unless otherwise noted.

Synthesis of Oligonucleotides Containing Methylphosphonate Linkages. Oligonucleotides containing methylphosphonate linkages were synthesized using standard phosphoramidite synthesis procedures on an Applied Biosystems 390 DNA/RNA synthesizer. Nucleoside phosphoramidites and methylphosphonamidites were purchased from Glenn Research (Sterling, VA). After synthesis, the DNA was deprotected and cleaved from the silica support by the addition of 0.5 mL of a 45:45:10 acetonitrile/ethanol/ammonium hydroxide mixture and allowed to incubate at room temperature for 30 min. Ethylenediamine (0.5 mL) was then added, and the DNA-containing solution was allowed to sit overnight at room temperature. The DNA-containing solution was separated from the silica support and dried under vacuum. After resuspension in 25 mM Tris-HCl (pH 7.5) (buffer A), the DNA was then purified from the failure products by high-performance liquid chromatography by injection onto a Dionex DNA Pac anion exchange column and eluted with a linear gradient from 10% buffer A to 90% buffer B [25 mM Tris-HCl (pH 7.5) and 1 M NaCl].

90mer oligonucleotide substrates used in the site transfer assays containing methylphosphonate linkages were first synthesized as smaller precursors, and then a three-piece ligation was performed to create the final product (Figure S1 of the Supporting Information). Sequences of the precursor oligonucleotides are listed in the Supporting Information. For ligation, piece 1 (1.5 nmol) and piece 2 containing methylphosphonate linkages (2 nmol) were first phosphorylated at the 5′ end by incubation with T4 PNK (New England Biolabs) at 37 °C in a single reaction mixture (~200 μL volume in 1× DNA ligase buffer, New England Biolabs). After inactivation of T4 PNK, Piece 3 (2 nmol) and the Splint (2 nmol) were then added to the reaction mix and hybridized by being heated to 95 °C for 5 min and allowed to cool slowly to room temperature by placing the heat block on the benchtop. Fresh ATP was then added to a final concentration of 1 mM along with T4 DNA ligase (New England Biolabs), and the reaction mixture was incubated at 37 °C overnight. The reaction mixture was then mixed with 50% formamide (final concentration), and the ligated product was purified by denaturing PAGE (Figure S1 of the Supporting Information).

Determination of DNA Dissociation Constants by Fluorescence Anisotropy. Binding of hUNG to nonspecific DNA was assessed using fluorescence anisotropy in a Spex Fluormax 3 fluorimeter at 37 °C using an excitation wavelength of 495 nm and an emission wavlength of 520 nm. Concentrated hUNG in the standard reaction buffer containing 50 nM labeled DNA was titrated into a cuvette containing 50 nM labeled DNA in reaction buffer to avoid dilution of the DNA during the titration. After each addition, the cuvette was placed in the fluorimeter and allowed to equilibrate for 2 min as the reading was found to stabilize after 60−90 s. For dissociation constants of >5 μM, K_D values were determined by diluting a concentrated solution of hUNG in reaction buffer and 50 nM labeled DNA with a solution of labeled DNA only. The forward titration was found to overlay titrations performed by dilution, indicating that anisotropy values were determined at equilibrium. Data were then fit to a single-site binding isotherm $[\text{anisotropy} = B_{max}[\text{hUNG}]_{free}/(K_D + [\text{hUNG}]_{free}) + B_{min}]$, where B_{max} and B_{min} are the maximal and minimal anisotropies, respectively, and it was assumed that the free DNA concentration equals the total (which is a valid assumption given that $K_D \gg [\text{DNA}]_{total}$).

Intramolecular Site Transfer Assay. Site transfer measurements were performed identically as before[9,11] with some modifications in the steps after reaction quenching to account for substrate and buffer differences. The DNA concentration in all site transfer measurements was 40 nM, and the hUNG concentration ranged from 10 to 20 pM under the standard reaction conditions and for the data presented in Figure 6 from 300 pM to 1.5 nM.

For methylphosphonate-containing duplexes (S5M and S6M), 30 pmol of the top and bottom DNA strands were 5′-end labeled with ^{33}P by incubation with T4 polynucleotide kinase and [γ-^{33}P]ATP in separate reactions. The reaction mixtures were then mixed and the strands hybridized by being heated to 95 °C for 10 min in a dry heat block followed by being slowly cooled to room temperature by placing the heat block on the benchtop. The hybridized DNA was then separated from the unicorporated [γ-^{33}P]ATP by gel filtration using P30 resin (Bio-Rad) and then desalted using P6 resin (Bio-Rad). Samples obtained before and after gel filtration were analyzed by native gel electrophoresis, where the percent recovery was calculated from imaging of the band densities, and the completeness of hybridization was confirmed. In general, the percent recovery was at least 80%. After reaction with hUNG and quenching by uracil DNA glycosylase inhibitor

protein (UGI, New England Biolabs), each individual reaction mixture was treated with the nicking enzyme Nt.BbvCI and APE1 endonuclease as previously described,[9,11] resulting in discrete double-stranded fragments corresponding to the hUNG reaction products. Each sample was then separated by electrophoresis on a 0.5 mm thick 10% native gel (19:1 bisacrylamide:acrylamide) run in 1× TBE buffer at 20 W in a model S2 sequencing gel for 1 h and 40 min without prerunning the gel.

For S6M^{ss}, the 5′ and 3′ ends were labeled by incubation with [γ-^{32}P]ATP and 3′-deoxyadenosine 5′-triphosphate (cordycepin 5′-triphosphate)-[α-^{32}P] using polynucleotide kinase and terminal transferase (New England Biolabs), respectively. As described above for the duplex substrates, after being radiolabeled, the unincorporated nucleotides and excess salts were removed by gel filtration using P30 and P6 resins (Bio-Rad). After reaction with hUNG and quenching, the resulting abasic sites were cleaved by the addition of 0.25 M ethylenediamine (pH 8.0) (final concentration) and then immediately heated to 95 °C for 5 min. Formamide containing both xylene cyanol and bromphenol blue was then added to a final concentration of 65%, and the samples were loaded onto a 10% denaturing gel (19:1 bisacrylamide:acrylamide).

For the duplex substrate S5 under physiological salt conditions [140 mM potassium glutamate, 200 μM $MgSO_4$, and 10 mM Na-HEPES (pH 7.5)], the uracil-containing strand was first labeled with ^{32}P at the 5′ and 3′ ends as described for S6M^{ss} above. The labeled strand was then hybridized to the complementary strand, and the unincorporated radiolabel was removed using P30 resin (Bio-Rad). The duplex substrate (40 nM) was then reacted with hUNG and the reaction quenched at various time points using UGI as described above. To each aliquot was added 3 μL of 0.25 M ethylenediamine (pH 8.0), and the reaction mixture was immediately heated to 95 °C for 5 min to cleave the DNA at the abasic sites. Formamide gel loading buffer was then added to a final concentration of 65%, and the samples were heated at 95 °C for an additional 3 min. The samples were immediately loaded onto a preheated 10% (19:1 bisacrylamide:acrylamide) denaturing gel to fully denature any residual structure.

Analysis of the Site Transfer Data. All gels were exposed to a storage phosphor screen and digitized using a phosphorimager. For each reaction time course, product band densities were quantified in QuantityOne using the box method. More details concerning data analysis are presented in the Results. All errors presented in the text are standard deviations derived from at least three independent measurements.

RESULTS

Approach. A method that allows measurement of the probability (P_{trans}) that hUNG will successfully transfer between two uracil sites embedded in a single DNA chain separated by a known distance using a sliding or hopping pathway was recently described (Figure 1a).[9] This is the first approach that allows dissection of the total transfer probability into the individual contributions from hopping (P_{hop}) and sliding (P_{slide}), where $P_{trans} = P_{hop} + P_{slide}$ (Figure 1).

The method requires quantitative site transfer probability measurements (see below) in the absence and presence of a small molecule trap of the enzyme. Inclusion of the trap (the free uracil base) serves to capture all enzyme molecules that have dissociated from the DNA during the process of transferring between the two uracil sites (i.e., the enzyme molecules that have hopped off the DNA). The trap has no effect on enzyme transfers that follow the sliding pathway because the binding site for the trap is blocked when hUNG is bound to nonspecific DNA. Separation of the two pathways (P_{hop} and P_{slide}) is possible because at zero concentration of trap transfer can occur by both hopping and sliding, but as the trap concentration increases, the hopping contribution diminishes in a hyperbolic fashion, ultimately approaching a limiting asymptote equal to P_{slide} (long dashed line in Figure 1b). If the site spacing is sufficiently large, no enzyme molecules will reach the second site without departing the DNA at least once, and transfer will be entirely ablated at high trap concentrations (short dashed line in Figure 1b). Conversely, at short site spacings, all transfers may occur by sliding and therefore will be impervious to the trap (solid line in Figure 1b).

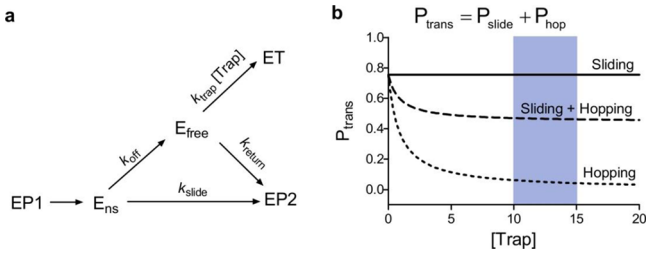

Figure 1. (a) "Molecular clock" approach that uses a small molecule inhibitor of hUNG (uracil) to trap enzyme molecules that have hopped off the DNA chain during transfer between two uracil target sites, while leaving sliding enzymes unperturbed.[9] Thus, this method allows quantitative determination of the individual contributions of hopping and sliding transfers (where the total transfer probability is $P_{trans} = P_{hop} + P_{slide}$). (b) Simulations showing the dependence of facilitated transfer (P_{trans}) on the concentration of the trap (based on the mechanism in panel a). As previously noted,[9] the probability of locating a site by hopping includes the probability that the enzyme initially falls off the DNA (P_{off}) as well as the probability that it returns to the same DNA chain (P_{return}) without being lost to bulk solution ($P_{hop} = P_{off}P_{return}$). The trap allows selective disruption of the hopping pathway because the probability that a hopping enzyme returns to the DNA chain decreases according to the equation $P_{return} = k_{return}/(k_{return} + k_{trap}[trap])$. The utility of this approach and the numerous control experiments that confirm its utility have been previously published.[9]

The reader is referred to ref 9 for a detailed description of the method, including control experiments that establish its utility for hUNG. The experimental observations that support the conclusion that uracil serves as a trap of a dissociated state of hUNG without disrupting DNA sliding are as follows: (i) Two pathways for transfer between substrate sites are observed (uracil insensitive and sensitive). (ii) The uracil concentration dependence of P_{trans} follows the expected hyperbolic kinetic behavior (Figure 1b), including the non-zero plateau value at short site spacings and high uracil concentrations, as would be expected for concurrent hopping and sliding. (iii) The site spacing dependencies of P_{slide} and P_{hop} are consistent with those expected for hopping and sliding pathways. That is, the probability for hopping (uracil sensitive) follows a $1/r$ dependence on site spacing, while the probability for sliding (uracil insensitive) shows a bp^2 dependence on site spacing. (iv) Transfer was completely eliminated at high uracil concentrations when the substrate sites were positioned on opposite DNA strands where an obligate dissociation−reassociation step is required for transfer. This was observed even though the opposite strand sites were closer in space than

dx.doi.org/10.1021/bi301561d | Biochemistry 2013, 52, 2526−2535

when they were positioned on the same strand. Additionally, at site spacings exceeding the sliding length, identical values of P_{trans} were previously observed for sites positioned on the same and opposite strands, consistent with hopping.[11] (v) The hopping pathway was highly sensitive to increases in ionic strength, while the sliding pathway was not.[9] (vi) High concentrations of uracil have no effect on the dissociation constant for nonspecific binding of UNG to DNA, but uracil blocks the catalytic activity of the enzyme.[9] These observations are consistent with the trap having no effect on sliding and acting solely by trapping the active site of the dissociated enzyme.

Calculating Site Transfer Probabilities. To determine the probabilities for facilitated site transfer by hUNG, we use an initial-rate, steady-state assay that quantifies the fraction of enzyme molecules that excise one uracil site (primary excision events) and then successfully transfer and excise the other uracil in the same DNA molecule (secondary excision events) (Figure 2a).[9,24,25] Primary or secondary uracil excision events will lead to discrete fragments of the doubly end-labeled DNA that may be resolved by polyacrylamide gel electrophoresis after postreaction sample processing (see Materials and Methods) (Figure 2b). If only primary excision events occur at site 1 or 2, the DNA fragments A + BC or AB + C will be produced in equal amounts with equal apparent velocities ($v_1 = v_2$) if each site reacts identically. However, if intramolecular transfer occurs, the larger AB and BC fragments will be efficiently converted into the smaller fragments A and C (as well as the unobserved B fragment) with velocities $v_{2\rightarrow1}$ (reflecting 2 → 1 transfers) and $v_{1\rightarrow2}$ (reflecting 1 → 2 transfers). It is worth noting that the initial rates for formation of fragments A and C depend on both primary and secondary events, and therefore, $v_{2\rightarrow1}$ and $v_{1\rightarrow2}$ are not necessarily equivalent to the initial rates of appearance of fragments A and C. In general, the qualitative hallmark of intramolecular transfer is the production of greater amounts of the secondary excision products A and C at the expense of the single-excision products AB and BC.[20,24]

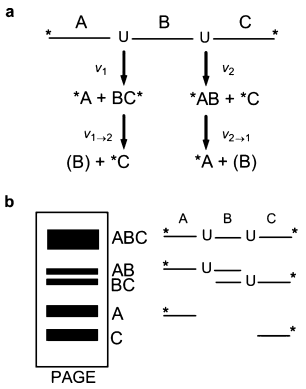

Figure 2. Site transfer assay. (a) Schematic of the site transfer assay in which a single strand of a duplex DNA substrate that contains two uracil sites is reacted with hUNG ([hUNG] ≪ [DNA]). After quenching, cleavage of the product abasic sites results in single-site (AB and BC) and double-site (A and C) product fragments (produced from intramolecular translocation events). Qualitatively, intramolecular translocation of hUNG is indicated by an excess of the A and C fragments under initial rate conditions (see the text). (b) Schematic of the reaction products as analyzed by gel electrophoresis. The intramolecular transfer efficiency is calculated from eq 1 using the band densities from the gel image (see the text).

The overall transfer probability (P_{trans}) may be precisely calculated from the time-dependent fragment concentrations. These concentrations are inserted into eq 1, which requires extrapolation to zero time to obtain the true transfer probability.[24] The basis for this equation can be easily understood: the denominator counts all excision events, and the numerator counts only secondary excision events.

$$P_{trans}^{obs} = ([A] + [C] - [AB] - [BC]) / ([A] + [C] + [AB] + [BC]) \quad (1)$$

Thus, the ratio reveals the fraction of all excision events that lead to successful transfers to the second site. (The term − [AB] − [BC] in the numerator corrects for the fact that fragments A and C can result from both primary excision events ABC → A + BC and ABC → AB + C, or secondary excision events AB → A + B and BC → B + C.) We find that this is a useful and straightforward analytical approach when there is no site preference for excision of the individual sites or no directional bias to transfer.[9,11] In the following paper (DOI: 10.1021/bi301562n), we use a modified analytical approach that is useful when a site excision or transfer bias is present.

Effects of Neutral Methylphosphonate (M) Substitutions on Nonspecific DNA Binding. Previous work suggested that a continuous DNA phosphate backbone was necessary and sufficient for DNA sliding because (i) hUNG

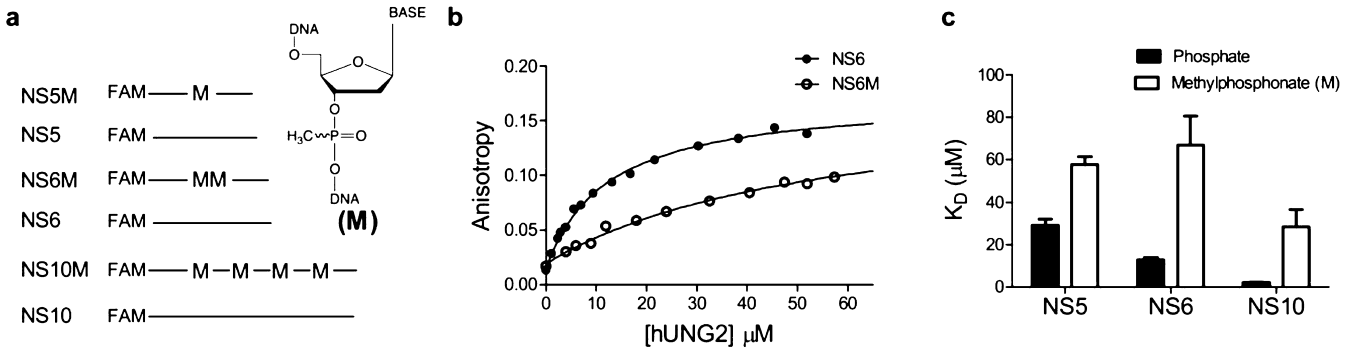

Figure 3. Substrate design and effects of methylphosphonate (M) substitutions on nonspecific DNA binding as measured using fluorescence anisotropy. (a) Design of 5′ fluorescein-labeled oligonucleotides containing all phosphodiester or methylphosphonate (M) linkages. NS5 and NS6 and their corresponding M-containing oligonucleotide sequences were chosen to match the intervening sequences in the uracil-containing substrate used in the site transfer assays. (b) Equilibrium hUNG binding to oligonucleotides NS6 and NS6M. (c) Summary of determined dissociation constants for hUNG and nonspecific DNA. Error bars represent means ± the standard deviation of at least three independent trials.

dx.doi.org/10.1021/bi301561d | Biochemistry 2013, 52, 2526−2535

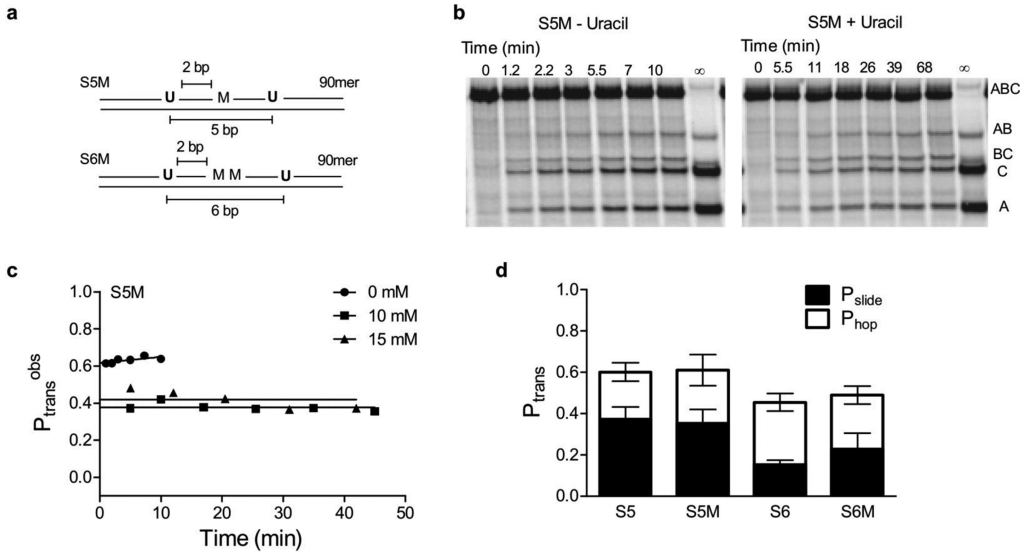

Figure 4. hUNG sliding and hopping is unaffected on double-stranded DNA substrates containing intervening neutral methylphosphonate (M) linkages. (a) Schematic of the substrates used (S5M and S6M). Methylphosphonate positioning was chosen so that the catalytic excision of uracil by hUNG is unaffected.[22,23] (b) Gel images of the site transfer products derived from S5M in the presence and absence of uracil. (c) Determination of P_{trans}, where the observed site transfer (P_{trans}^{obs}, eq 1) is calculated at each time point and linearly extrapolated to time zero to determine the true site transfer value (P_{trans}). Values at 10 and 15 mM uracil were identical, indicating measurements were made within the plateau region depicted in Figure 1b. (d) Summary of the site transfer properties of hUNG for double-stranded methylphosphonate-containing DNA substrates compared to the all phosphodiester versions. Data for S5 and S6 were reported previously and are shown for comparison.[9] Values are equal to means ± the standard deviation of at least three trials at 0 mM uracil and six at high uracil concentrations (three each at 10 and 15 mM uracil).

sliding occurred only between uracil sites that were positioned on the same strand in duplex DNA and (ii) sliding between uracil sites was observed on single-stranded DNA (ssDNA) substrates [ref 9 and the following paper (DOI: 10.1021/bi301562n)]. To begin to explore the role of phosphate backbone charge on DNA sliding, the effects of neutral M substitutions on nonspecific DNA binding were first determined using fluorescence anisotropy measurements (Figure 3). Three 5′ fluorescein-labeled DNA constructs that contained mixed diastereomer M linkages at one or more positions were investigated and then compared with the corresponding all-phosphodiester versions (Figure 3a). The M−DNA constructs shown in Figure 3a were chosen to match the intervening DNA strand segments used in the site transfer measurements described below (NS5M and NS6M) and also to evaluate the effect of removing as many as four phosphate charges (NS10M). Using single DNA strands as models for the intervening sequences in duplex DNA is justified because (i) structural studies indicate that hUNG primarily interacts with the phosphate backbone on the single strand of DNA that connects the two target bases,[26] (ii) hUNG is known to slide along a single strand in duplex DNA [ref 9 and the following paper (DOI: 10.1021/bi301562n)], and (iii) M substitutions in a single strand of duplex DNA still allow binding to the other strand and would complicate the interpretation of equilibrium dissociation constants.

Binding measurements revealed that single or multiple M substitutions in single-stranded DNA decreased the binding affinity (K_d) of hUNG compared to those of matched all-phosphodiester controls (Figure 3b,c). The 2 fold-effect of a single M substitution in the center of a 5mer strand (NS5M and NS5; $\Delta\Delta G$ = 0.42 kcal/mol) was increased 5-fold in the 6mer strand containing two M substitutions (NS6M; $\Delta\Delta G$ = 1.01 kcal/mol, or ∼0.5 kcal/mol per M linkage). Similarly, the 10mer strand containing four methylphosphonates (NS10M) showed a 14-fold deficit in binding ($\Delta\Delta G$ = 1.52 kcal/mol, or ∼0.4 kcal/mol per M linkage). Qualitatively, these results demonstrate that the removal of phosphate charge has a damaging effect on nonspecific DNA binding and raise the expectation that if site transfer by hUNG requires interaction with the phosphate backbone, the removal of these interactions should diminish successful sliding between two uracil sites. We defer to the Discussion possible further physical interpretations of the effects of M substitution on nonspecific DNA binding.

Sliding of hUNG Does Not Require a Continuous Polyanion DNA Strand. To address the question of whether a continuous backbone charge is a requirement for sliding along duplex DNA, we synthesized two 90mer M-substituted DNA substrates containing M linkages on the DNA strand connecting the two uracils (Figure 4a). The intervening nonspecific DNA strand that connects the two uracil sites in these substrates corresponds exactly to the sequence of NS5M or NS6M described above. Importantly, the substrates in Figure 4a were constructed with uracil spacings of 5 and 6 bp (S5M and S6M, respectively) because it has been previously shown that 40 and 20% of the hUNG site transfers occur by a sliding pathway at these spacings when uninterrupted phosphodiester linkages are present.[9] In addition, we took care to position the M linkages far enough from the uracil sites such that the footprint of the specific hUNG catalytic complex does not overlap these positions. This aspect of the substrate design is critical because it has been shown that specific M substitutions within two nucleotides of the uracil site can have a large damaging effect on catalysis ($\Delta\Delta G$ of up to 10 kcal/mol).[22,23]

We measured P_{trans}, P_{slide}, and P_{hop} for S5M and S6M and compared these values to those previously measured for the analogous phosphodiester substrates S5 and S6 (Figure 4).[9] As described above, measurements of P_{trans} were obtained in the absence of the uracil trap, and measurements of P_{slide} were obtained in the presence of 10 and 15 mM trap (the two values

were identical, confirming that the transfer measurements were in the plateau region depicted in Figure 1b). For all of the data, P_{slide} is reported as the average value obtained at 10 and 15 mM uracil (n = 3 for each concentration), and P_{hop} is the difference between P_{trans} and P_{slide}. Representative transfer data for S5M in the absence and presence of the uracil trap show a significant degree of intramolecular transfer as revealed by excess A and C fragments (Figure 4b). Addition of 10 or 15 mM uracil trap leads to a reduction in the number of successful transfer events, but transfer is not entirely ablated, indicating that a sliding pathway is present (Figure 4b). Extrapolation to time zero using eq 1 shows that P_{trans} = 0.61 ± 0.08 and P_{slide} = 0.35 ± 0.07 for S5M, which are values indistinguishable from those previously reported for S5 (Figure 4c,d). In addition, there was no difference between the transfer parameters of S6M containing two intervening M linkages and the all-phosphodiester analogue S6 (Figure 4d). The transfer parameters for these phosphodiester and M-substituted substrates are summarized in Figure 4d, from which we conclude that ablating as many as one-third of the intervening negative charges connecting the two uracil sites has no measurable effect on P_{trans}, P_{slide}, or P_{hop}.

We next examined M linkages in the context of transfer of hUNG on single-stranded DNA using a ssDNA substrate that contained two M linkages analogous to the duplex S6M (S6M^{ss}). S6M^{ss} was designed to have minimal secondary structure and to have no more than two adjacent adjacent Watson−Crick pairings to eliminate potential secondary structure (Figure S2 of the Supporting Information). The data for S6M^{ss} are summarized in Figure 5 and show that M linkages have no effect on site transfer compared to that of the all-phosphodiester ssDNA substrate S5^{ss}. Comparing S6^{ss} to S5^{ss} is justified because P_{slide} for ssDNA has a flat dependence with site spacing between 5 and 10 nucleotides[9] [see also the following paper (DOI: 10.1021/bi301562n)].

The absence of a requirement for a continuous phosphate charge in sliding or hopping between two closely spaced sites in double-stranded DNA (dsDNA) or ssDNA is striking in comparison with the damaging effect of M substitutions on the K_m for a uracil-containing substrate ($\Delta\Delta G$ ~ 1−4 kcal/mol depending on position),[22] the large and highly stereospecific 5−10 kcal/mol effects of single M substitutions on the activation barriers for uracil excision in single strand or dsDNA,[22,23] and the significant effects of M substitution on nonspecific DNA binding reported above. These differences suggest that the rapid kinetic process of nonspecific sliding does not involve the same phosphate backbone interactions observed in crystal structures of nonspecific and specific complexes between hUNG and DNA.[26,27]

hUNG Site Transfer Using Physiological Ion Concentrations. Site transfer measurements published previously have been studied under conditions where the NaCl concentration ranged from 22 to 72 mM. In this range, sliding was found to be insensitive to salt, but hopping was fully ablated at salt concentrations exceeding 42 mM.[9] However, it is desirable to evaluate these parameters under conditions that more closely mimic the intracellular ion concentrations. For this purpose, we use a buffer consisting of 140 mM potassium glutamate, 10 mM Na-HEPES (pH 7.5), and 200 μM $MgSO_4$.

Measurements of equilibrium nonspecific DNA binding and hUNG catalytic activity under these conditions were first made. Compared to that under low-ionic strength conditions, the equilibrium dissociation constant for nonspecific binding was

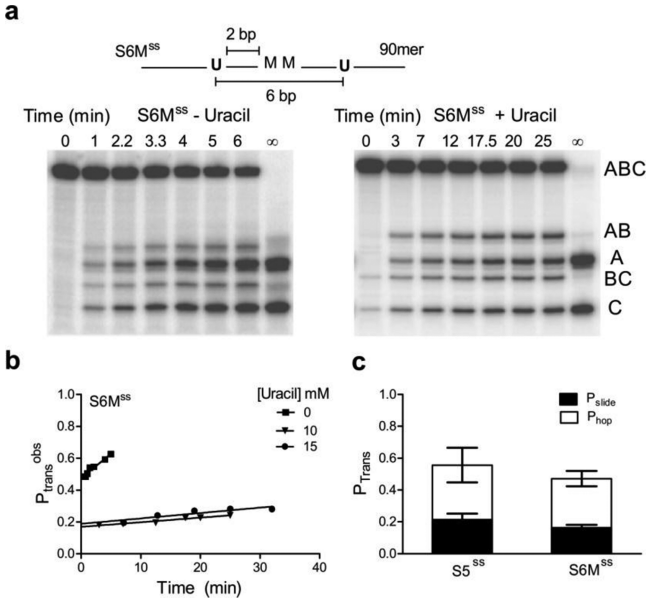

Figure 5. hUNG sliding on ssDNA is unaffected by methylphosphonate substitutions. (a) Gel images of the site transfer assay in the presence and absence of uracil for S6M^{ss}, which contains two intervening M substitutions. We note the presence of a small amount of cleavage in the time zero lane (<1%). This was found to be the result of the commercially available terminal deoxynucleotidyltransferase used in the 3′ end labeling reaction having a very small amount of uracil DNA glycosylase activity over the >2 h incubation at 37 °C, likely from copurification. These background bands were determined to have no effect on the site transfer calculations. (b) Linear extrapolation of P_{trans}^{obs} for S6M^{ss} in the presence and absence of uracil to determine P_{trans}. (c) Comparison of the site transfer measurements of S6M^{ss} to that of the all phosphodiester substrate S5^{ss}. Comparison with S5^{ss} is reasonable because site transfer by sliding on ssDNA shows no change for site spacings between 5 and 10 nucleotides (see the text).

increased ~100-fold (from 0.82 ± 0.26 to 85 ± 19 μM) (Figure S3a of the Supporting Information). Similarly, the catalytic activity of hUNG for a 90mer DNA duplex substrate containing a single uracil site was reduced ~300-fold under these conditions with a measured k_{cat}/K_m of 1 × 10^6 M^{-1} s^{-1} (Figure S3b of the Supporting Information). This value may be compared with the previously measured k_{cat}/K_m of 3.4 × 10^8 M^{-1} s^{-1} for the identical substrate at a low ionic strength. We note that accurate determinations of k_{cat} and K_m were not possible under physiological salt conditions, but a good estimate of k_{cat}/K_m could be obtained from the linear increase in rate using 0−4 μM substrate (Figure S3b of the Supporting Information). Most of the effect on activity can be assigned to K_m because the maximal observed rates under physiological salt concentrations approached the k_{cat} value of 5 s^{-1} under low-salt conditions.[9]

Site transfer measurements were then taken using the physiological buffer with duplex substrate S5, which contains two uracils positioned 5 bp apart (Figure 6). At this spacing, intramolecular site transfer was still observed (P_{trans} = 0.20 ± 0.04). The transfer probability was similar at high uracil concentrations (P_{slide} = 0.16 ± 0.06), indicating that within the error of the measurements all transfers occur by sliding, although P_{slide} was reduced compared to the value at low ionic strengths (P_{slide} = 0.37 ± 0.06). This result matches the previous finding that the hopping pathway is eliminated with a

dx.doi.org/10.1021/bi301561d | Biochemistry 2013, 52, 2526−2535

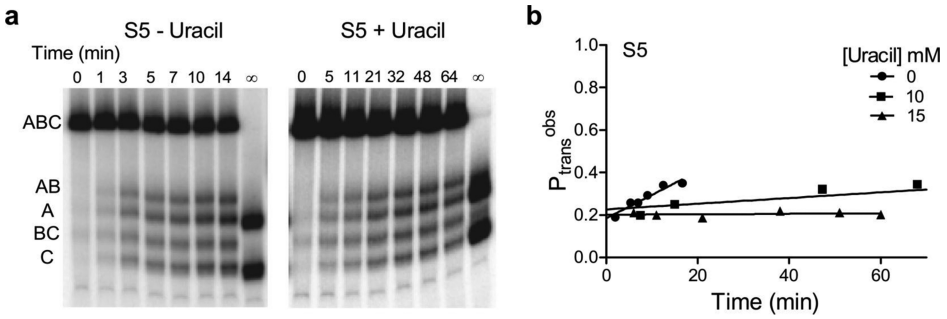

Figure 6. Site transfer measurements of hUNG under approximated physiological ionic strength conditions [140 mM potassium glutamate, 10 mM Na-HEPES (pH 7.5), and 200 μM $MgSO_4$]. (a) Gel images of the raw site transfer measurements in the presence and absence of uracil. (b) Determination of P_{trans} by linear extrapolation. The values are the same in the presence and absence of uracil, indicating that site transfer occurs entirely by sliding under these high-salt conditions.

salt concentration of 42 mM while sliding persists unabated at the same concentration.[9] Thus, despite the 100-fold decrease in nonspecific binding affinity under mock physiological conditions, short-range sliding of hUNG on DNA can still occur. These findings imply that the binding interface of the sliding form of hUNG is immune to invasion by salt ions. This observation is consistent with the inability of the uracil trap to access the active site of hUNG during the process of sliding.

DISCUSSION

Different Effects of M Substitution on Nonspecific DNA Binding, DNA Translocation, and Uracil Excision. Comparison of the divergent effects of methylphosphonate (M) substitutions on nonspecific DNA binding, translocation between uracil sites, and catalysis by UNG leads to the conclusion that the requirements for a charged phosphate group in these processes are very different. Previous studies in which stereospecific M substitutions were made in single-stranded and duplex substrates of UNG have revealed that substitutions at the +1, −1, and −2 phosphates surrounding the uracil site ($5'p^{+1}Up^{-1}Np^{-2}N3'$) result in stereospecific 10−10^8-fold damaging effects on catalysis.[22,23] Most of these large effects were attributed to the beneficial energetic effects of the anionic phosphate groups with respect to stabilization of the glycosyl cation transition state. The previously measured damaging effects of single M substitutions on the ground-state Michaelis complex were not stereospecific and were smaller than the effects on the activation barrier (i.e., K_m effects were in the range of 10−100-fold).[22,23] The even smaller damaging effect of a single M substitution on nonspecific DNA binding [~2-fold (Figure 3c)] would suggest that the nonspecific complex differs in its interactions with the phosphate backbone from the Michaelis complex. Despite the apparent differences between these complexes revealed by M substitution, the high-resolution crystal structures of the specific and nonspecific hUNG−DNA complexes show that the same phosphate groups form hydrogen bonds with neutral serine or histidine side chains, or backbone amide groups, and that there are few cationic groups ≤3.3 Å from phosphate oxygens (Figure 7).[26] Thus, taken together, these energetic measurements suggest that as the enzyme moves forward along the reaction coordinate it forms increasingly important electrostatic interactions with the phosphate backbone. The interesting exception, as shown in this work, is the transient state for DNA sliding that apparently has no requirement for an uninterrupted charged phosphate chain.

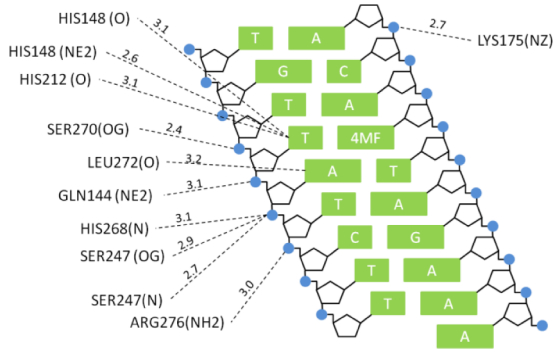

Figure 7. DNA interactions of hUNG nonspecifically bound to a destabilized thymine base pair (Protein Data Bank entry 2OXM;[27], 4MF = 4-methylindole). Residues shown have a nitrogen or oxygen atom <3.3 Å from a nitrogen or oxygen of a DNA base or a phosphate oxygen of the DNA backbone.

What is the physical basis for the different effects of M substitution on nonspecific binding and DNA translocation? Although M substitution has an only minor effect on the structural parameters of B-DNA,[28−30] this substitution can change duplex hydration patterns[29,31] and quite possibly reduce the ion count in the cloud loosely associated with the DNA.[32,33] Thus, these indirect outcomes of M substitution can make unique mechanistic interpretations of the observed effects elusive. In the case presented here, the small damaging effects of M substitution on nonspecific DNA binding (0.5 kcal/mol per substitution) could reflect direct disruption of the backbone hydrogen bonding in the complex (Figure 7), or a reduction in minor groove hydration waters or ions around the neutral patch.[29,31] If these indirect effects prevail, then the reduction in binding affinity upon M substitution could arise from a smaller favorable entropy change resulting from fewer water molecules or ions being released to bulk solution upon complexation.[34] Although such indirect effects might provide viable explanations for the reduced binding affinity of hUNG for M-substituted DNA, they do not reasonably account for the absence of an effect of M substitution on DNA sliding because sliding occurs in a kinetic event after the ion cloud has been dispersed.

The absence of a functional requirement for a continuous negatively charged backbone in site translocation strongly suggests that the sliding form of hUNG cannot simply involve translocation of the crystallographic conformation of hUNG along DNA.[26,27,35,36] Rather, the data would suggest that the sliding conformation of hUNG is an open state that interacts loosely with the DNA backbone, with perhaps intervening

dx.doi.org/10.1021/bi301561d | Biochemistry 2013, 52, 2526−2535

water molecules (but not solute ions) that would serve to shield charge. This view of a loose, transiently bound conformation is consistent with CPMG NMR dynamic measurements indicating that UNG oscillates between open and closed forms on the millisecond time scale when bound to nonspecific DNA.[37] The open form was proposed to function in stochastic sliding along the DNA chain, and the closed form resembles the crystallographic conformation, allowing hUNG to interrogate the integrity of base pairs. Indeed, a two-state conformational change has been postulated as a general mechanism for site-specific DNA binding proteins to overcome the search-speed/stability paradox,[3,4,38] and recent structural evidence obtained with other DNA glycosylases suggests evidence of more than one conformation involved in search and recognition by these enzymes.[12,13] The findings reported here provide a first glimpse at the electrostatic properties of this transient state of hUNG.

Boundary Estimates for 1D Translocation on Duplex DNA. Employing the measured values for the average lifetime of hUNG on nonspecific DNA (τ_{bind} = 3 ms) and its mean sliding length (L_{slide} = 4.2 bp), we previously used eq 2 to estimate the 1D diffusion constant (D_1) of hUNG on nonspecific duplex DNA ($D_1 = 6 \times 10^3$ bp^2 s^{-1} = 7×10^{-4} μm^2 s^{-1}).[9] This value was several orders of magnitude below the theoretical upper limit (~10^7 bp^2 s^{-1} or ~1 μm^2 s^{-1}).[5,39,40]

$$D_1 = \frac{L_{slide}^{\ 2}}{\tau_{bind}} \qquad (2)$$

This calculation assumes that the entire bound lifetime of hUNG is available for DNA sliding. However the current data, which require the presence of at least two nonspecific states of hUNG, also require that only a fraction of the bound lifetime be available for sliding (i.e., the time spent in the open state). An estimated lower limit for the population of the transient sliding state may be estimated on the basis of the sensitivity of the NMR relaxation dispersion dynamic measurements previously performed on the hUNG-nonspecific DNA complex.[37] This methodology would not be able to detect a transient sliding state with a population of less than ~5% of the total, setting a lower limit for the time spent sliding of 0.05 × 3 ms (≥0.15 ms). It is difficult to set an upper boundary, but it must be considerably less than 3 ms. Using eq 2 and this lower limit for the sliding time, we calculate an upper limit for D_1 of ≤10^5 bp^2 s^{-1}. Thus, the previous and current estimates place D_1 in the range of ~10^4 to 10^5 bp^2 s^{-1}. Given this refined two-state view of sliding by hUNG, we suggest that the sliding state resembles the transition state for DNA dissociation. However, instead of falling off the DNA chain, the enzyme closes on the DNA and completes a sliding transfer. This viewpoint of short-range sliding as an aborted transition state for DNA dissociation differs considerably from other characterizations of protein sliding whereby the protein moves isoenergetically along the surface of the DNA.[41−43] These aspects of the hUNG search mechanism are depicted in the model presented in Figure 8.

Search and Recognition in the Cell Nucleus. Under optimal low-salt reaction conditions, hUNG is an evolutionarily optimized enzyme with a catalytic power that vastly exceeds that of any other DNA glycosylase.[1] However, under conditions that more closely mimic the intracellular ionic environment, its ability to bind nonspecific DNA is severely hampered by a factor of around 100-fold, which exerts a profound effect on the mechanism of site location. One major ramification of the ionic strength effect on nonspecific DNA binding is that hopping becomes a less productive pathway. Each time hUNG dissociates from the DNA chain under high-salt conditions, there will be a reduced probability that a reassociation attempt will result in a productive binding event. Thus, many more attempts will have to be made, which will result in an increase in the search time contributed by hopping. In contrast, DNA sliding is largely refractory to increases in ionic strength, and the search time resulting from sliding will remain largely unchanged. This important property of sliding, even over the short ranges traveled by hUNG, is essential for increasing the level of coverage of the genome and for the ultimate detection of damage (Figure 8). An additional consideration within the nuclear environment is the effect of crowding, as well as excluded volume effects.[44,45] Such factors could favor compact sliding states and also increase the contribution of hopping because of the high local concentration of DNA chains. Consideration of such effects requires improved experimental models for search and recognition.

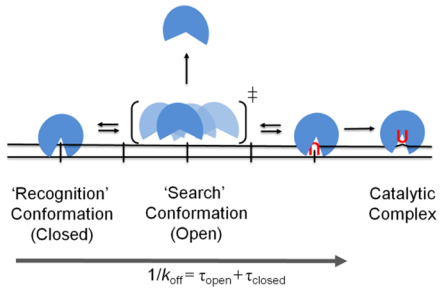

Figure 8. Two-state model for hUNG sliding on nonspecific DNA. In this model, hUNG exists in a highly populated "closed" recognition conformation that makes multiple interactions with the phosphate backbone as observed in crystallographic studies, and also a transient mobile "open" sliding conformation that makes few or no interactions with the phosphate backbone (this work). It is reasonable to view the open state as the aborted transition state preceding DNA dissociation. The open state, which must be present at least 5% of the total bound lifetime (see the text), allows for fast movement on the DNA while also allowing time for recognition of uracil bases when they are encountered.

■ ASSOCIATED CONTENT

Supporting Information

Supplemental methods and three supporting figures: schematic description of the splint ligation strategy used to synthesize 90mer DNA substrates containing methylphosphonate linkages (Figure S1), mFold output showing the lack of secondary structure for the single-strand substrate S6M^{ss} (Figure S2), and steady-state kinetic parameters of hUNG and nonspecific DNA binding at physiological salt concentrations (Figure S3). This material is available free of charge via the Internet at http://pubs.acs.org.

■ AUTHOR INFORMATION

Corresponding Author

*E-mail: jstivers@jhmi.edu. Phone: (410) 502-2758. Fax: (410) 955-3023.

Funding

J.D.S was supported by an American Heart Association predoctoral fellowship AHAPRE12040394. This work was supported by National Institutes of Health Grant GM056834 (J.T.S.).

Notes

The authors declare no competing financial interest.

■ ACKNOWLEDGMENTS

We thank Dr. David Draper for valuable discussions on this work.

■ REFERENCES

(1) Stivers, J. T., and Jiang, Y. L. (2003) A mechanistic perspective on the chemistry of DNA repair glycosylases. *Chem. Rev. 103*, 2729−2759.
(2) Friedman, J. I., and Stivers, J. T. (2010) Detection of Damaged DNA Bases by DNA Glycosylase Enzymes. *Biochemistry 49*, 4957−4967.
(3) Mirny, L., Slutsky, M., Wunderlich, Z., Tafvizi, A., Leith, J., and Kosmrlj, A. (2009) How a protein searches for its site on DNA: The mechanism of facilitated diffusion. *J. Phys. A: Math. Theor. 42*, 434013.
(4) Slutsky, M., and Mirny, L. A. (2004) Kinetics of protein-DNA interaction: Facilitated target location in sequence-dependent potential. *Biophys. J. 87*, 4021−4035.
(5) Berg, O. G., Winter, R. B., and Hippel, Von, P. H. (1981) Diffusion-driven mechanisms of protein translocation on nucleic acids. 1. Models and theory. *Biochemistry 20*, 6929−6948.
(6) Halford, S. E., and Marko, J. F. (2004) How do site-specific DNA-binding proteins find their targets? *Nucleic Acids Res. 32*, 3040−3052.
(7) Gowers, D. M., Wilson, G. G., and Halford, S. E. (2005) Measurement of the contributions of 1D and 3D pathways to the translocation of a protein along DNA. *Proc. Natl. Acad. Sci. U.S.A. 102*, 15883−15888.
(8) Hedglin, M., and O'Brien, P. J. (2010) Hopping Enables a DNA Repair Glycosylase To Search Both Strands and Bypass a Bound Protein. *ACS Chem. Biol. 5*, 427−436.
(9) Schonhoft, J. D., and Stivers, J. T. (2012) Timing facilitated site transfer of an enzyme on DNA. *Nat. Chem. Biol. 8*, 205−210.
(10) Blainey, P. C., van Oijen, A. M., Banerjee, A., Verdine, G. L., and Xie, X. S. (2006) A base-excision DNA-repair protein finds intrahelical lesion bases by fast sliding in contact with DNA. *Proc. Natl. Acad. Sci. U.S.A. 103*, 5752−5757.
(11) Porecha, R. H., and Stivers, J. T. (2008) Uracil DNA glycosylase uses DNA hopping and short-range sliding to trap extrahelical uracils. *Proc. Natl. Acad. Sci. U.S.A. 105*, 10791−10796.
(12) Qi, Y., Nam, K., Spong, M. C., Banerjee, A., Sung, R.-J., Zhang, M., Karplus, M., and Verdine, G. L. (2012) Strandwise translocation of a DNA glycosylase on undamaged DNA. *Proc. Natl. Acad. Sci. U.S.A. 109*, 1086−1091.
(13) Setser, J. W., Lingaraju, G. M., Davis, C. A., Samson, L. D., and Drennan, C. L. (2012) Searching for DNA lesions: Structural evidence for lower- and higher-affinity DNA binding conformations of human alkyladenine DNA glycosylase. *Biochemistry 51*, 382−390.
(14) Dunn, A. R., Kad, N. M., Nelson, S. R., Warshaw, D. M., and Wallace, S. S. (2011) Single Qdot-labeled glycosylase molecules use a wedge amino acid to probe for lesions while scanning along DNA. *Nucleic Acids Res. 39*, 7487−7498.
(15) Terakawa, T., Kenzaki, H., and Takada, S. (2012) p53 Searches on DNA by Rotation-Uncoupled Sliding at C-Terminal Tails and Restricted Hopping of Core Domains. *J. Am. Chem. Soc. 134*, 14555−14562.
(16) Leith, J. S., Tafvizi, A., Huang, F., Uspal, W. E., Doyle, P. S., Fersht, A. R., Mirny, L. A., and van Oijen, A. M. (2012) Sequence-dependent sliding kinetics of p53. *Proc. Natl. Acad. Sci. U.S.A. 109*, 16552−16557.
(17) limpm, A. G., Yeykal, C. C., Robertson, R. B., and Greene, E. C. (2006) Long-distance lateral diffusion of human Rad51 on double-stranded DNA. *Proc. Natl. Acad. Sci. U.S.A. 103*, 1221−1226.
(18) Senavirathne, G., Jaszczur, M., Auerbach, P. A., Upton, T. G., Chelico, L., Goodman, M. F., and Rueda, D. (2012) Single-stranded DNA scanning and deamination by APOBEC3G cytidine deaminase at single molecule resolution. *J. Biol. Chem. 287*, 15826−15835.
(19) Hammar, P., Leroy, P., Mahmutovic, A., Marklund, E. G., Berg, O. G., and Elf , J. (2012) The lac repressor displays facilitated diffusion in living cells. *Science 336*, 1595−1598.
(20) Stanford, N. P., Szczelkun, M. D., Marko, J. F., and Halford, S. E. (2000) One- and three-dimensional pathways for proteins to reach specific DNA sites. *EMBO J. 19*, 6546−6557.
(21) Werner, R. M., Jiang, Y. L., Gordley, R. G., Jagadeesh, G. J., Ladner, J. E., Xiao, G., Tordova, M., Gilliland, G. L., and Stivers, J. T. (2000) Stressing-Out DNA? The Contribution of Serine−Phosphodiester Interactions in Catalysis by Uracil DNA Glycosylase. *Biochemistry 39*, 12585−12594.
(22) Jiang, Y. L., Ichikawa, Y., Song, F., and Stivers, J. T. (2003) Powering DNA Repair through Substrate Electrostatic Interactions. *Biochemistry 42*, 1922−1929.
(23) Parker, J. B., and Stivers, J. T. (2008) Uracil DNA glycosylase: Revisiting substrate-assisted catalysis by DNA phosphate anions. *Biochemistry 47*, 8614−8622.
(24) Terry, B. J., Jack, W. E., and Modrich, P. (1985) Facilitated diffusion during catalysis by EcoRI endonuclease. Nonspecific interactions in EcoRI catalysis. *J. Biol. Chem. 260*, 13130−13137.
(25) Porecha, R. H., and Stivers, J. T. (2008) Uracil DNA glycosylase uses DNA hopping and short-range sliding to trap extrahelical uracils. *Proc. Natl. Acad. Sci. U.S.A. 105*, 10791−10796.
(26) Slupphaug, G., Mol, C. D., Kavli, B., Arvai, A. S., Krokan, H. E., and Tainer, J. A. (1996) A nucleotide-flipping mechanism from the structure of human uracil-DNA glycosylase bound to DNA. *Nature 384*, 87−92.
(27) Parker, J. B., Bianchet, M. A., Krosky, D. J., Friedman, J. I., Amzel, L. M., and Stivers, J. T. (2007) Enzymatic capture of an extrahelical thymine in the search for uracil in DNA. *Nature 449*, 433−437.
(28) Thiviyanathan, V., Vyazovkina, K. V., Gozansky, E. K., Bichenchova, E., Abramova, T. V., Luxon, B. A., Lebedev, A. V., and Gorenstein, D. G. (2002) Structure of Hybrid Backbone Methylphosphonate DNA Heteroduplexes: Effect of R and S Stereochemistry. *Biochemistry 41*, 827−838.
(29) Hamelberg, D., Williams, L. D., and Wilson, W. D. (2002) Effect of a neutralized phosphate backbone on the minor groove of B-DNA: Molecular dynamics simulation studies. *Nucleic Acids Res. 30*, 3615−3623.
(30) Williams, L. D., and Maher, L. J., III (2013) Electrostatic mechanisms of DNA deformation. *Annu. Rev. Biophys. Biomol. Struct. 29*, 497−521.
(31) Hausheer, F. H., Rao, B. G., Saxe, J. D., and Singh, U. C. (1992) Physicochemical properties of (R)- vs (S)-methylphosphonate substitution on antisense DNA hybridization determined by free energy perturbation and molecular dynamics. *J. Am. Chem. Soc. 114*, 3201−3206.
(32) Bai, Y., Chu, V. B., Lipfert, J., Pande, V. S., Herschlag, D., and Doniach, S. (2008) Critical Assessment of Nucleic Acid Electrostatics via Experimental and Computational Investigation of an Unfolded State Ensemble. *J. Am. Chem. Soc. 130*, 12334−12341.
(33) Das, R., Mills, T., Kwok, L., Maskel, G., Millett, I., Doniach, S., Finkelstein, K., Herschlag, D., and Pollack, L. (2003) Counterion Distribution around DNA Probed by Solution X-ray Scattering. *Phys. Rev. Lett. 90*, 188103.
(34) Privalov, P. L., Dragan, A. I., and Crane-Robinson, C. (2011) Interpreting protein/DNA interactions: Distinguishing specific from non-specific and electrostatic from non-electrostatic components. *Nucleic Acids Res. 39*, 2483−2491.
(35) Mol, C. D., Arvai, A. S., Slupphaug, G., Kavli, B., Alseth, I., Krokan, H. E., and Tainer, J. A. (1995) Crystal structure and mutational analysis of human uracil-DNA glycosylase: Structural basis for specificity and catalysis. *Cell 80*, 869−878.
(36) Parikh, S. S., Mol, C. D., Slupphaug, G., Bharati, S., Krokan, H. E., and Tainer, J. A. (1998) Base excision repair initiation revealed by crystal structures and binding kinetics of human uracil-DNA glycosylase with DNA. *EMBO J. 17*, 5214−5226.

(37) Friedman, J. I., Majumdar, A., and Stivers, J. T. (2009) Nontarget DNA binding shapes the dynamic landscape for enzymatic recognition of DNA damage. *Nucleic Acids Res. 37*, 3493−3500.
(38) Zhou, H.-X. (2011) Rapid search for specific sites on DNA through conformational switch of nonspecifically bound proteins. *Proc. Natl. Acad. Sci. U.S.A. 108*, 8651−8656.
(39) Schurr, J. M. (1979) The one-dimensional diffusion coefficient of proteins absorbed on DNA: Hydrodynamic considerations. *Biophys. Chem. 9*, 413−414.
(40) Bagchi, B., Blainey, P. C., and Xie, X. S. (2008) Diffusion Constant of a Nonspecifically Bound Protein Undergoing Curvilinear Motion along DNA. *J. Phys. Chem. B 112*, 6282−6284.
(41) Berg, O. G., and Hippel, von, P. H. (1985) Diffusion-controlled macromolecular interactions. *Annu. Rev. Biophys. Biophys. Chem. 14*, 131−160.
(42) Winter, R. B., Berg, O. G., and von Hippel, P. H. (1981) Diffusion-driven mechanisms of protein translocation on nucleic acids. 3. The *Escherichia coli* lac repressor-operator interaction: Kinetic measurements and conclusions. *Biochemistry 20*, 6961−6977.
(43) Winter, R. B., and von Hippel, P. H. (1982) How do genome-regulatory proteins locate their DNA target sites? *Trends Biochem. Sci. 7*, 52−55.
(44) Zhou, H.-X., Rivas, G., and Minton, A. P. (2008) Macromolecular crowding and confinement: Biochemical, biophysical, and potential physiological consequences. *Annu. Rev. Biophys. 37*, 375−397.
(45) Schreiber, G., Haran, G., and Zhou, H.-X. (2009) Fundamental aspects of protein-protein association kinetics. *Chem. Rev. 109*, 839−860.